Kinetics and Mechanism of the Heterogeneous Oxidation of Ethane and Ethylene on Samarium(III) Oxide

V. T. Amorebieta[†] and A. J. Colussi*[,‡]

Contribution from the Department of Chemistry, University of Mar del Plata, 7600-Mar del Plata, Argentina, and Department of Physical Chemistry, Faculty of Exact and Natural Sciences, University of Buenos Aires, 1428-Buenos Aires, Argentina

Received April 18, 1996[⊗]

Abstract: The rates and products of the purely heterogeneous oxidations of C_2H_6(g) and C_2H_4(g) on Sm_2O_3 in the presence of O_2(g) were investigated in a very low-pressure flow reactor by on-line molecular beam mass spectrometry, about 1000 ± 100 K. Ethane is oxidized to ethyl radicals, which undergo unimolecular decomposition into (C_2H_4 + H) or further oxidation to CO. C_2H_4 oxidation leads to CO as initial product, that is subsequently converted into CO_2. Steady state rates are proportional to $k_i'([O_2]) \times [C_2H_n]$, with $k_i'([O_2]) = k_i \times (K_i[O_2])^{1/2}/\{1+(K_i[O_2])^{1/2}\}$ (i = 3, 4 for n = 6, 4, respectively), which is consistent with the direct oxidation of hydrocarbons on surface oxygen species in dissociative equilibrium with O_2(g). Alternate or simultaneous measurement of the oxidation rates for C_2H_6, C_2H_4, and CH_4, the latter proportional to $k_1'[CH_4]$, on the same Sm_2O_3 sample as function of $[O_2]$ and temperature, led to the following expressions: $\log (k_3/k_1) = -(0.14 \pm 0.30) + (663 \pm 300)/T$ (I), $\log(k_4/k_1) = (1.08 \pm 0.35) - (646 \pm 365)/T$ (II), $\log (K_1/\mathrm{nM}^{-1}) = (2.76 \pm 0.46) - (4363 \pm 468)/T$ (III), $\log (K_3/\mathrm{nM}^{-1}) = (1.85 \pm 0.22) - (4123 \pm 260)/T$ (IV), $\log(K_4/\mathrm{nM}^{-1}) = (5.31 \pm 0.65) - (6480 \pm 647)/T$ (V) (nM = 10^{-9}M), that are independent of catalyst mass, active area, or morphology. Equations I−V imply that ethane and ethylene are oxidized faster than methane at all relevant temperatures. Although the activation energies, $E_4 > E_1 > E_3$, correlate with the corresponding BDE(C−H) energies suggesting a common H-atom abstraction mechanism, the *A*-factor for the oxidation of ethylene is about tenfold larger. Oxidations occur on distinguishable O_s species generated by endothermic, exentropic O_2 chemisorption involving cooperative participation of the solid.

Introduction

The partial catalytic oxidation of methane on selected metal oxides is the most promising route for the conversion of vast worldwide reserves of natural gas into more valuable chemical feedstocks.[1−8] Under typical operating conditions CH_4/O_2 mixtures at atmospheric pressure flow over oxide catalysts at temperatures ca. 1000 K. It is widely agreed that the flameless oxidation process that takes place under such conditions is initiated by the production of methyl radicals:[7,9−12]

$$CH_4(g) + \alpha_xO_s \rightarrow \beta CH_3(g) + (1-\beta)CO_x + \{2 - (3\beta/2)\}H_2O \quad (1)$$

followed by CH_3(g) dimerization

$$2CH_3(g) + M \rightarrow C_2H_6(g) + M \quad (2)$$

or further oxidation, either in the gas-phase or on the catalyst.[12−15] The rather drastic conditions required to drive reaction 1 at appreciable rates represent a formidable obstacle in the task of kinetically controlling the production of the thermodynamically favored waste carbon oxides.[1,12,16−18] Hundreds of publications attest to the empirical attempts directed at overcoming the apparently insurmountable ceiling of 25% for C_2-yields,[19,20] which—at current prices—is considered the threshold for an economically viable process.[21] As usual, research efforts have focused on the identification of suitable catalyst materials, rather than on the kinetics and mechanism of these processes.[22]

We have recently shown that carbon oxides are not primary products of methane oxidation on samaria, a prototype catalyst.[14] Hence, the loss of C_2 selectivity must be a consequence of the secondary oxidation of methyl radical intermediates or of the

[†] University of Mar del Plata.
[‡] University of Buenos Aires.
[⊗] Abstract published in *Advance ACS Abstracts*, September 15, 1996.

(1) (a) Keller, G. E.; Bashin, M. M. *J. Catal.* **1982**, *73*, 9. (b) Krylov, O. V. *Catal. Today* **1993**, *18*, 209.
(2) Tonkovich, A. L.; Carr, R. W.; Aris, R. *Science* **1993**, *262*, 221.
(3) Krylov, O. V. *Kinet. Catal.* **1993**, *34*, 18.
(4) Jiang, Y.; Yentekakis, I. V.; Vayenas, C. G. *Science* **1994**, *264*, 1563.
(5) (a) Olah, G. A.; Molnar, A. *Hydrocarbon Chemistry*; Wiley: New York, 1994. (b) Crabtree, R. H. *Chem. Rev.* **1995**, *95*, 987.
(6) Kalenik, Z.; Wolf, E. *Catalysis, A Specialist Periodical Report*; The Royal Society of Chemistry: 1993; Vol. 10, p 154, and references therein.
(7) Lunsford, J. H.; Cisneros, M. D.; Hinson, P. G.; Tong, T.; Zhang, H. *Faraday Discuss. Chem. Soc.* **1989**, *87*, 13, and references therein.
(8) Amenomiya, Y.; Birss, V. I.; Goledzinowski, M.; Galuszka, J.; Sanger, A. R. *Catal. Rev.-Sci. Eng.* **1990**, *32*, 163, and references therein.
(9) Tong,Y.; Lunsford, J. H. *J. Am. Chem. Soc.* **1991**, *113*, 4741.
(10) Feng, Y.; Niiranen, J.; Gutman, D. *J. Phys. Chem.* **1991**, *95*, 6558, and 6564.
(11) (a) Amorebieta, V. T.; Colussi, A. J. *J. Phys. Chem.* **1989**, *93*, 5155. (b) Amorebieta, V. T.; Colussi, A. J. *J. Phys. Chem.* **1988**, *92*, 4576.
(12) Amorebieta, V. T.; Colussi, A. J. *J. Am. Chem. Soc.* **1995**, *117*, 3856.
(13) Grela, M. A.; Amorebieta, V. T.; Colussi, A. J. *J. Phys. Chem.* **1992**, *96*, 7013.
(14) Colussi, A. J.; Amorebieta, V. T. *J. Phys. Chem.* **1995**, *99*, 13291.
(15) Grela, M. A.; Colussi. A. J *Twenty-Fifth International Symposium on Combustion, The Combustion Institute*; 1994; p 733.
(16) Shi, C.; Rosynek, M. P.; Lunsford, *J. Phys. Chem.* **1994**, *98*, 8371.
(17) McCarty, J. G.; McEwen, A. B.; Quinlan, M. A. *New Developments in Selective Oxidation*; Centi, G., Trifiro, F., Eds.; Elsevier: New York, 1990; p 405.
(18) (a) Labinger, J. A.; Ott, K. C. *J. Phys. Chem.* **1987**, *91*, 2682. (b) Labinger, J. A. *Catal. Lett.* **1988**, *1*, 371.
(19) Parkyns, N. D.; Warburton, C. I.; Wilson, J. D. *Catal. Today* **1993**, *18*, 385.
(20) Hutchings, G. J.; Joyner, R. *Chemistry Industry* **1991**, 575.
(21) Fox, J. M. *Catal. Rev.-Sci. Eng.* **1993**, *35*, 169.
(22) Hutchings, G. J.; Scurrell, M. S.; Woodhouse, J. R. *J. Chem. Soc., Chem. Commun.* **1987**, 1862.

S0002-7863(96)01273-5 CCC: $12.00

C_2 products themselves.[16] Considering that at atmospheric pressures the essentially unselective gas-phase oxidations compete successfully with heterogeneous reactions on the catalyst surface,[8,23] the source of selectivity must be sought in surface events.[6,13,15] It follows that the heterogeneous processes of interest are best studied in isolation by working at sufficiently low pressures.[10−12] This caveat qualifies the results of experiments performed at atmospheric pressure, where gas-phase oxidation generally masks the outcome of gas-solid catalytic reactions.

Clearly, in order to ascertain the largest possible yield of C_2 hydrocarbons in the catalytic oxidation of methane in a rational way it is necessary to investigate not only the oxidation of methane but also the rates and products of the heterogeneous oxidations of intermediates and products.[6,16−18,24−29] We recently resumed such a program, having completed studies on the oxidation of methyl radicals, both in the gas phase and on samaria.[12,13] In this paper we report kinetic data and product analysis for the heterogeneous oxidation of ethane and ethylene on the same catalyst:

$$C_2H_6(g) + \gamma_x O_s \rightarrow \delta C_2H_5(g) + 2(1-\delta)CO_x + (3-2.5\delta)H_2O \quad (3)$$

$$C_2H_4(g) + \gamma_\epsilon O_s \rightarrow 2\epsilon CO + 2(1-\epsilon)CO_2 + 2H_2O \quad (4)$$

Since only relative rates are actually required to model the catalytic oxidation of methane at steady state,[12,30] the typical uncertainties associated with the active areas of solid catalysts are circumvented by normalizing all rates to the rate of methane oxidation, measured under identical conditions. In this manner we generate a self-consistent kinetic dataset that is uniquely suited for the task at hand.[30] We found that ethane and ethylene are oxidized faster than methane at all accessible temperatures, being about three times more reactive at 1000 K. The differences of activation energies, $(E_3 - E_1) < 0 < (E_4 - E_1)$, correlate with the corresponding C−H bond energies, BDE(C_2H_5-H) < BDE(CH_3-H) < BDE(C_2H_3-H),[31,32] suggesting that C−H bond breaking is a common feature of the transition states for the heterogeneous oxidations of hydrocarbons on metal oxides. The similar *A*-factors of reactions 1 and 3 imply further analogies. In contrast, the considerably larger value for the oxidation of the olefin: $A_4/A_1 \approx 10$, points to the oxidation of a precursor surface intermediate, rather than a direct Eley−Rideal mechanism.[27,28] The thermodynamic parameters characterizing the endothermic O_2-chemisorptions producing the O_s centers active in reactions 1 and 3 are also similar but considerably different from those associated with the species responsible for the oxidation of ethylene or methyl radicals.[12] This finding is direct evidence of the existence of distinguishable catalytic sites and offers a firm clue in the quest for selectivity. It seems that this is the first time such information—essential for a fundamental understanding of the performance of catalyst oxides in the oxidative dimerization of methane—is reported.

Experimental Section

The inlet of a heatable flow reactor (fused silica, cylindrical, 5 cm diameter, 90 cm^3) was connected to the vacuum manifold and its outlet to an analytical mass spectrometer (Extrel). The reactor was operated in the effusive flow regime, characterized by mass-dependent residence times: $t_i = 1/k_{ei} = 7.5\ (M_i/T)^{1/2}$ s, and gas-wall collision frequencies: $\omega_i = 6.0 \times 10^3\ (T/M_i)^{1/2}\ s^{-1}$ (where the M_i's are molecular masses in daltons).[33,34] Thin beds of catalyst samples (ca. 240 mg) could be rapidly (within 1 s) inserted or removed along the axis of the reactor by means of a homemade all-quartz sliding holder. Considering that all hydrocarbons share the same port and that mean free paths at prevalent pressures are of the order of a few centimeters, i.e., that the reactor is well stirred, we assume that all gases flow over the catalyst bed under identical conditions. Gas-catalyst collision frequencies were calculated from the expression: $\omega_{is} = [A_s/(A_s + A_r)] \times 6.0 \times 10^3\ (T/M_i)^{1/2}\ s^{-1}$, where A_s is the visual area of the catalyst layer, and A_r is the inner area of reactor walls. We favor the use of visual areas, rather than BET values,[9] because under present conditions mean free paths are much longer than pore sizes and adsorption of gases other than O_2 can be ignored. Mixtures of ethane or ethylene (0.06−2 nmol s^{-1}) and O_2 (0.2−173 nmol s^{-1}) steadily circulated through the reactor, corresponding to overall pressures <5 mTorr. The fast mass spectrometric detection system (40 eV electron impact ionization) for the continuous and simultaneous monitoring of reactants and products has been described in detail previously.[12,14] It consists of a differential pumping chamber, in which a molecular beam is created from the gases exiting the reactor, a collimating orifice, and a second chamber housing a variable speed chopper, an axial electron impact ionizer, and a quadrupole mass analyzer. Signals from the electron multiplier were amplified, fed to a lock-in amplifier, filtered, and acquired by a personal computer for further analysis. Mass scans could be typically programmed to sample each peak for 200 ms or longer, at a frequency of 10 Hz or smaller, depending on the time constant of the lock-in amplifier, and the S/N ratio. Samarium(III) oxide (Aldrich), was conditioned under air at 1073 K for about 8 h before use. This treatment results in partial sintering, which we found necessary to prevent catalyst blowoff in the evacuated reactor. Methane, oxygen, and argon (high purity, AGA Argentina), ethylene (Matheson, CP), and ethane (>99%, generously supplied by Petroquímica Bahía Blanca, Argentina) were used as received.

Results and Discussion

Reaction Products. Based on our previous work on methane,[11] we anticipated that the heterogeneous oxidation of ethane on samaria, reaction 3, would be initiated by an H-atom abstraction step analogous to, but faster than reaction 1

$$C_2H_6(g) + O_s = C_2H_5(g) \quad (5)$$

followed by the fast gas-phase unimolecular decomposition or surface oxidation of ethyl radicals:[27,35]

$$C_2H_5(g) + M = C_2H_4(g) + H(g) + M \quad (6a)$$

$$C_2H_5(g) + O_s = CO_x(g) \quad (6b)$$

In Figure 1a−c we present the mass spectra of a reacting C_2H_6 (39.6 nanomolar = 2.4 mTorr)/O_2 (25.5 nanomolar = 1.6 mTorr) mixture over 240 mg of Sm_2O_3 at 990 K. Figure 1a corresponds to the difference between the mass spectrum of the mixture in the presence of the catalyst minus a fraction of the mass spectrum acquired in its absence at the same temperature. The spectrum of the unreacted mixture was attenuated in order

(23) Mackie, J. C. *Catal. Rev.-Sci. Eng.* **1991**, *33*, 169, and references therein.
(24) Morales, E.; Lunsford, J. H. *J. Catal.* **1989**, *118*, 255.
(25) Choudhary, V. R.; Rane, V. H. *J. Catal.* **1992**, *135*, 317.
(26) Burch, R.; Tsang, S. C. *Appl. Catal.* **1990**, *65*, 259.
(27) Driscoll, D. J.; Lunsford, J. H. *J. Phys. Chem.* **1985**, *89*, 4415.
(28) Aika, K.-I.; Lunsford, J. H. *J. Phys. Chem.* **1978**, *82*, 1794.
(29) Conway, S. J.; Lunsford, J. H. *J. Catal.* **1991**, *131*, 513.
(30) Amorebieta, V. T.; Colussi, A. J. Submitted for publication to *J. Phys. Chem.*
(31) Colussi, A. J. *Chemical Kinetics of Small Organic Radicals*; Alfassi, Z. B., Ed.; CRC: Boca Raton, FL, 1988; Vol. I, p 25.
(32) Kaiser, E. W.; Wallington, T. J. *J. Phys. Chem.* **1996**, *100*, 4111.
(33) (a) Amorebieta, V. T.; Colussi, A. J. *J. Phys. Chem.* **1982**, *86*, 2760. (b) Colussi, A. J.; Zabel, F.; Benson, S. W. *Int. J. Chem. Kinet.* **1977**, *9*, 161. It is possible to detect ethyl radicals mass spectrometrically at 15 eV in a very low pressure reactor at high temperatures, in the absence of reactive pathways other than unimolecular decomposition.
(34) Golden, D. M.; Spokes, G. N.; Benson, S. W. *Angew. Chem., Int. Ed. Engl.* **1973**, *12*, 534.

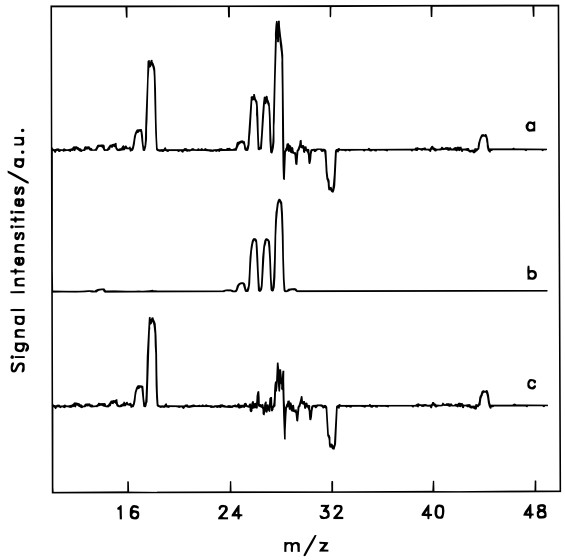

Figure 1. Products of ethane oxidation. (a) 40 eV mass spectrum of a reacting mixture [$F(C_2H_6) = 2.7$ nmol s^{-1}, $F(O_2) = 1.7$ nmol s^{-1}] in the presence of 240 mg of Sm_2O_3 at 990 K, minus a fraction of the one acquired in its absence so as to obliterate the signal at $m/z = 30$; (b) the mass spectrum of C_2H_4; (c) corresponds to the difference (a − b).

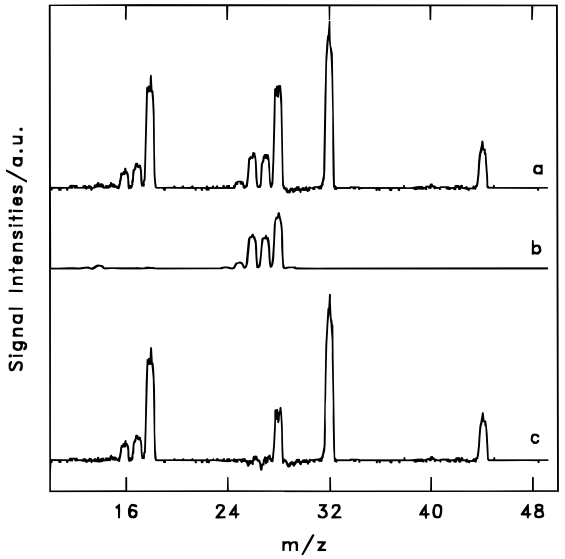

Figure 2. Products of ethane oxidation. Same as Figure 1, but for a larger oxygen flow rate: $F(O_2) = 15.4$ nmol s^{-1}.

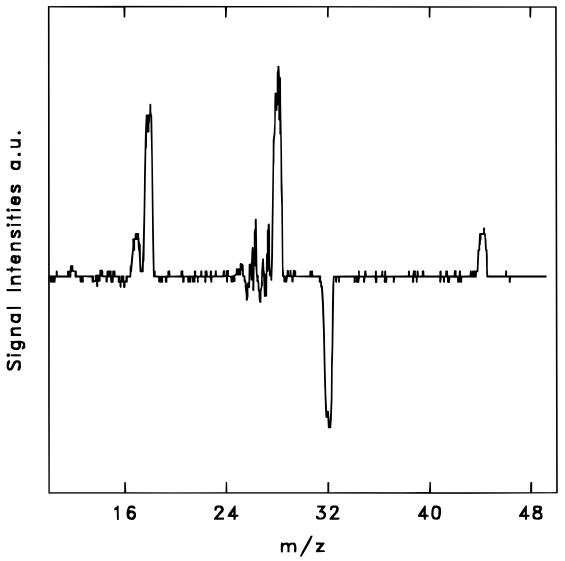

Figure 3. Products of ethylene oxidation. 40 eV mass spectrum of a reacting mixture [$F(C_2H_4) = 3.7$ nmol s^{-1}, $F(O_2) = 2.1$ nmol s^{-1}] in the presence of 240 mg of Sm_2O_3 at 1000 K, minus a fraction of the one acquired in its absence so as to obliterate the signal at $m/z = 28$.

to obliterate the signal at $m/z = 30$ ($C_2H_6^+$) in Figure 1a. This procedure is intended to cancel out daughter ion contributions from the mass spectrum of unreacted ethane to the signals at $m/z = 26-29$. We observe a net consumption of O_2 ($m/z = 32$) and the formation of C_2H_4 ($m/z = 26$, 27 and 28), H_2O ($m/z = 18$), CO_2 ($m/z = 44$), and possibly CO ($m/z = 28$). Since only C_2H_4 can contribute to the fragments at $m/z = 26$ and 27 in Figure 1a, we subtracted the mass spectrum of neat ethylene (Figure 1b) from Figure 1a. The resulting spectrum is displayed in Figure 1c. Clearly, a residual signal at $m/z = 28$ remains, which is ascribed to carbon monoxide. Notice that after factoring out the contribution of ethane, the vanishingly small $m/z = 29$ signal in Figure 1a reveals the absence of ethyl radicals in the gas mixture effusing from the reactor.[33]

Suitable calibrations of relative molar flow response factors f, $f^{30}_{C_2H_6}/f^{28}_{C_2H_4} = 0.30$, $f^{44}_{CO_2}/f^{28}_{C_2H_4} = 1.23$, $f^{44}_{CO_2}/f^{28}_{CO} = 2.00$, allow us to quantify the yields of the different products. The f^i_x factor for the i fragment in the mass spectrum of X is defined by the relationship, $I^i_x = f^i_x k_{e,x}[X]_{ss}$, where I^i_x is the signal intensity of the corresponding fragment at a given electron energy, $k_{e,x}$ is the escape rate constant of X (see experimental section) and $[X]_{ss}$ is its steady state molar concentration within the reactor. An equivalent definition can be given in terms of the molar flow rates F_x: $I^i_x = f^i_x(F_x/V)$, where V is the reactor volume. The results of the experiment of Figure 1 correspond to the conversion of 23% ethane into 81% ethylene, 20% CO, and 5% CO_2, which add up to a nearly quantitative carbon balance.

Figure 2a−c displays the results for a oxygen richer mixture: C_2H_6 (39.6 nanomolar)/O_2 (231 nanomolar) also at 990 K. About 33.3% ethane is now oxidized with the formation of 32% C_2H_4, 39% CO, and 18% CO_2, i.e., about 89% of total carbon is accounted for. Clearly, these results strongly suggest that carbon oxides are not primary products of reaction 3, i.e., that $\delta \approx 1$. This conclusion confirms some, but not all, of the previous high-pressure experimental results.[16,24,29,36] The answer to the question of whether CO_x species derive from the heterogeneous oxidations of C_2H_5 radicals or C_2H_4 requires information on the rates and products of ethylene heterogeneous oxidation. This issue is dealt with in the Appendix.

Product analysis in the oxidation of ethylene is more straightforward. In Figure 3 we show the difference between the mass spectrum of a lean reaction mixture ($[C_2H_4]_0 = 52$ nanomolar, $[O_2]_0 = 239$ nanomolar) after passing over the catalyst, minus the mass spectrum of the feed, scaled as to cancel out C_2H_4 contributions to the $m/z = 26$ and 27 signals. Notice the residual signal at $m/z = 32$ (O_2^+), an artifact of the scaling procedure due to the different mass spectrometric response factors of C_2H_4 and O_2. About 31% C_2H_4 is consumed leading to the formation of water ($m/z = 18$), 76% carbon monoxide ($m/z = 28$) and 24% carbon dioxide ($m/z = 44$). In a richer mixture ($[C_2H_4]_0 = 52$ nanomolar, $[O_2]_0 = 30.7$ nanomolar), the net consumption of O_2 becomes apparent as a negative signal

(35) Westley, F.; Frizzell, D. H.; Herron, J. T.; Hampson, R. F.; Mallard, W. G. NIST Chemical Kinetics Database 17, Version 5.0; National Institute of Standards and Technology: Gaithersburg, MD, 1993.

(36) (a) Roos, J. A.; Korf, S. J.; Veehof, R. H. J.; Van Ommen, J. G.; Ross, J. R. H. *Appl. Catal.* **1989**, *52*, 147 (b) Otsuka, K.; Abdel-Aziz, A. J. *Inorg. Chim. Acta* **1987**, *132*, 123, infer that CO_2 is mainly formed in ethane oxidation.

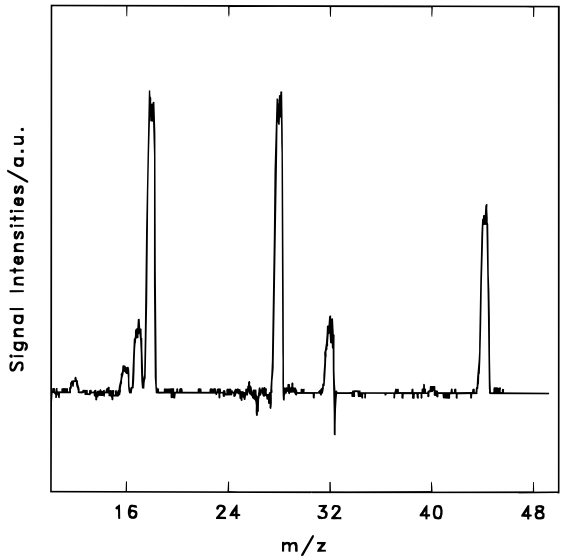

Figure 4. Same as in Figure 3, but for a larger oxygen flow rate: $F(O_2) = 16.0$ nmol s^{-1}.

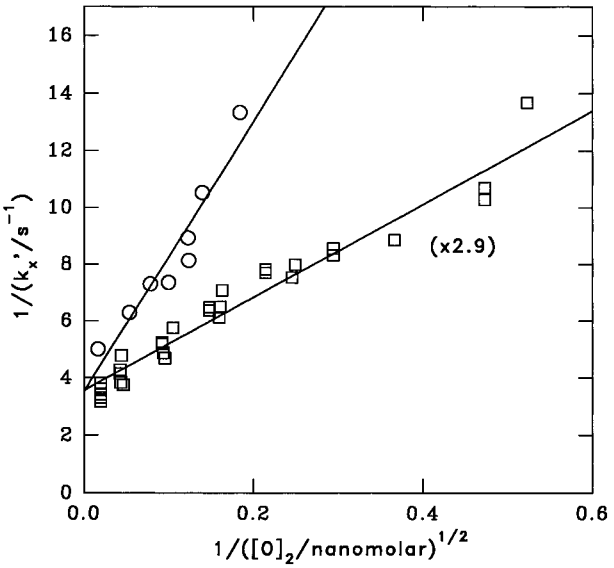

Figure 5. Kinetic data for methane and ethane oxidation. The reciprocals of the pseudo-first-order rate constants ($1/k_x'$) vs the reciprocal of the square root of steady state O_2(g) concentrations within the reactor in the presence of 240 mg of Sm_2O_3 at 1000 K. Circles: CH_4 oxidation; squares: C_2H_6 oxidation.

at $m/z = 32$ in the difference mass spectrum. The conversion of 3% C_2H_4 produces a smaller 10% CO_2 yield vs 90% CO (Figure 4). These observations indicate that CO is the primary product of ethylene heterogeneous oxidation. We were unable to detect vinyl radicals ($m/z = 27$), in accord with previous studies.[27]

Kinetic and Thermodynamic Data

Pseudo-first-order rate constants for the heterogeneous oxidations of methane, k_1', ethane, k_3', and ethylene, k_4', at constant $[O_2]$, were calculated from the expression

$$k_x' = k_{e,x} f/(1 - f) \qquad \text{(VI)}$$

where the rate constant for the escape of methane, ethane, and ethylene are given by $k_{e,16} = (3.34 \times 10^{-2})T^{1/2}$ s^{-1}, $k_{e,30} = (2.43 \times 10^{-2})T^{1/2}$ s^{-1}, and $k_{e,28} = (2.52 \times 10^{-2})T^{1/2}$ s^{-1}, respectively, $f = (I_{woc} - I_{wc})/I_{woc}$, is the fraction of reactant oxidized on the catalyst, and I_{wc} and I_{woc} are the steady state intensities of the

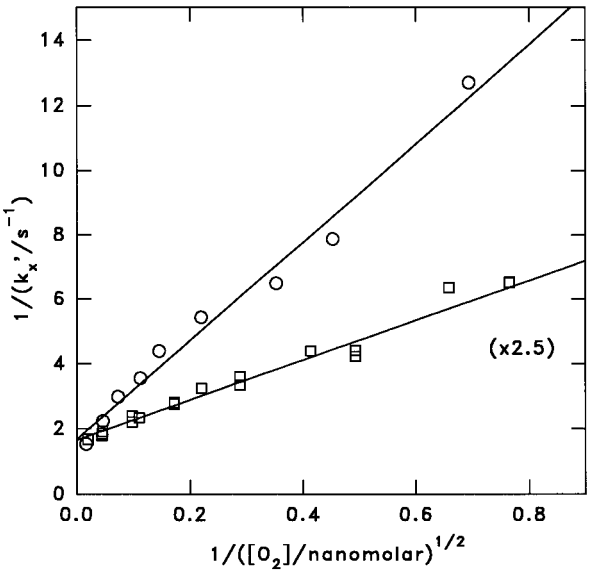

Figure 6. Same as Figure 5 but at 1100 K.

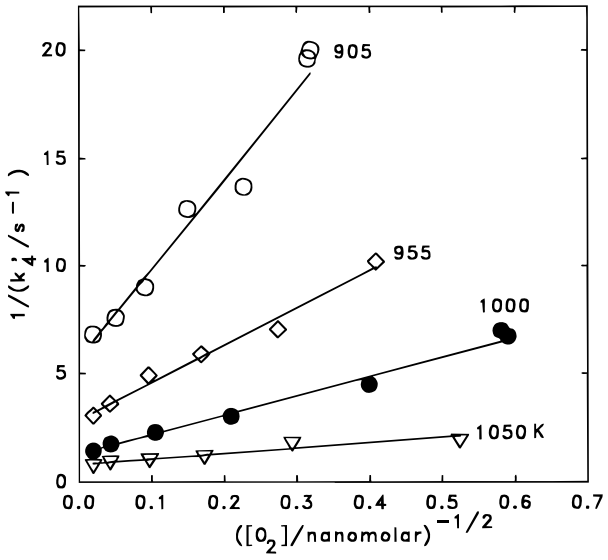

Figure 7. Kinetic data for ethylene oxidation. The reciprocals of the pseudo-first order rate constants ($1/k_4'$) vs the reciprocal of the square root of steady state O_2(g) concentrations within the reactor in the presence of 240 mg of Sm_2O_3 at various temperatures.

$m/z = 16$, 28, or 30 signals, with and without catalyst, respectively. We verified that k_x' values calculated from eq VI are actually independent of hydrocarbon flow rates in the range 0.06−2.0 nmol/s, confirming the assumed first-order kinetics, i.e., that $d[X]/dt = -k_x'[X]$. However, the derived k_x' values depend on $[O_2]$ in a nonlinear manner, in line with previous results from our laboratory and elsewhere.[10−12] The data in Figures 5−7 clearly show that *(1) ($1/k_x'$) values measured for all hydrocarbons on the same oxide sample depend linearly on $[O_2]^{1/2}$, (2) ethane and ethylene react faster than methane below 2000 K, and (3) k_3' and k_4' are less sensitive to $[O_2]$ than k_1'.*

We have previously shown, in our studies of methane oxidation on Li/MgO and Sm_2O_3, that the linearity of such plots is consistent with the following overall rate law[10−12]

$$-d[X])/dt = k_x[X]K_x^{1/2}[O_2]^{1/2}/(1+K_x^{1/2}[O_2]^{1/2}) \qquad \text{(VII)}$$

i.e., with: $1/k_x' = (1/k_x) \times \{1 + (K_x^{-1/2}[O_2]^{-1/2})\}$. This type of kinetics, in turn, implies that the reactive surface oxygen species O_s that appear in steps 1, 3, and 4 are in dissociative

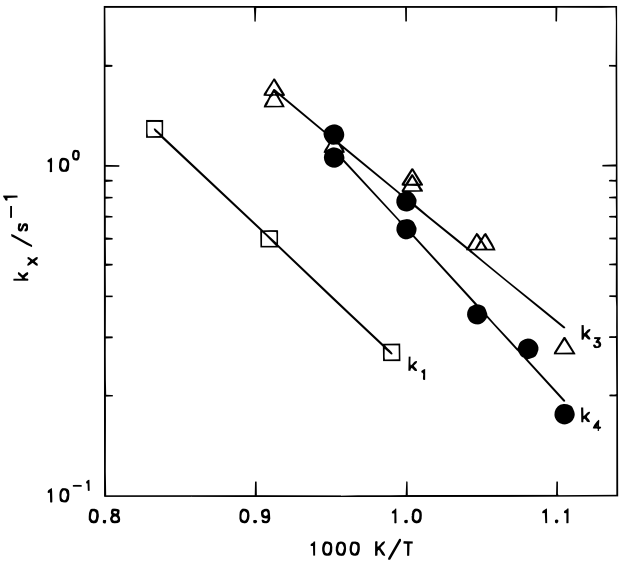

Figure 8. Arrhenius plots for the rate constants of methane k_1, ethane k_3, and ethylene k_4 oxidations over 240 mg of Sm_2O_3. Rate constants are the reciprocals of the intercepts in Figures 5−7. Their ratios are independent of catalyst mass or active areas.

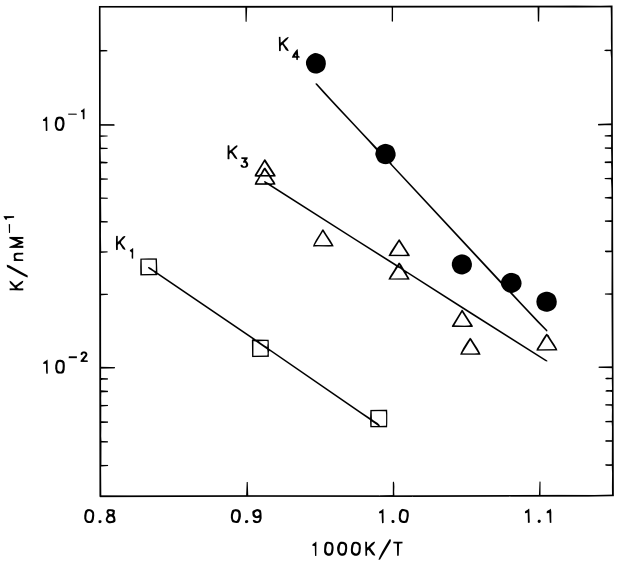

Figure 9. van't Hoff plots for the phenomenological equilibrium constants of O_2(g) dissociative chemisorption on Sm_2O_3. They were obtained as the squares of the reciprocals of the slopes in Figures 5−7. K_1, K_3, and K_4 correspond to the formation of chemisorbed oxygen species participating in reactions 1, 3, and 4, respectively. Notice that O_2(g) chemisorption is *endothermic* in all cases.

equilibrium with O_2(g), or, alternatively, with a O_{2s} species whose concentration is proportional to O_2(g)[12]

$$O_2(g) \rightleftharpoons O_{2s} \qquad (7)$$

$$O_{2s} \rightleftharpoons O_2(g) \qquad (-7)$$

$$O_{2s} \leftrightarrow 2O_s \qquad (8)$$

According to this analysis, the reciprocals of the intercepts in Figures 5, 6, and 7 yield the desired k_1, k_3, and k_4 rate constants of the pseudoelementary oxidation processes. From the corresponding slopes, one can derive the equilibrium constants for O_2-chemisorption: $K_x = K_7K_8$. Arrhenius plots for the kinetic constants are shown in Figure 8. In Figure 9 we present the van't Hoff plots for the equilibrium constants. The

Table 1. Kinetic and Thermodynamic Data for the Heterogeneous Oxidations of Methane, Ethane, and Ethylene on Samaria[a]

$\log (k_1/s^{-1}) = (3.74 \pm 0.03) - (4352 \pm 31)/T$
$\log (k_3/s^{-1}) = (3.59 \pm 0.26) - (3689 \pm 266)/T$
$\log (k_4/s^{-1}) = (4.81 \pm 0.32) - (4996 \pm 315)/T$
$\log (k_3/k_1) = (-0.15 \pm 0.29) + (663 \pm 300)/T$
$\log (k_4/k_1) = (1.08 \pm 0.35) - (646 \pm 365)/T$
$\log (K_1/10^9\ M^{-1}) = (1.85 \pm 0.22) - (4123 \pm 260)/T$
$\log (K_3/10^9\ M^{-1}) = (2.76 \pm 0.46) - (4363 \pm 468)/T$
$\log (K_4/10^9\ M^{-1}) = (5.31 \pm 0.65) - (6480 \pm 647)/T$

[a] Subscripts 1, 3, and 4 correspond to methane, ethane, and ethylene, respectively. Absolute values of rate constants k_1, k_3, and k_4 measured on 240 mg Sm_2O_3. Only their ratios are independent of catalyst mass or active area.

derived least squares parameters, and their standard deviations, are collected in Table 1. The activation energies of the elementary rate determining steps, $E_1 = 19.9$, $E_3 = 16.9$, and $E_4 = 22.9$ kcal/mol, respectively, should not be confused with activation energies calculated from overall rates measured at constant (or variable!) $[O_2]$.[10]

The similar activation energies for the three reactions point to a common mechanism, probably involving H-atom abstraction by the surface. Actually, the nearly constant activation energy increments, $(E_4 - E_1) \approx (E_1 - E_3) \approx 3$ kcal/mol, nicely correlate with the sequence, BDE(C_2H_5-H) = 100.5, BDE(CH_3-H) = 105.1, and BDE(C_2H_3-H) = 110.5 kcal/mol.[31,32] The relatively larger A_4 value is significant and may be indicative of the oxidation of a bound surface intermediate rather than a direct Eley−Rideal mechanism. Previous investigations by Lunsford et al. have shown that C_2H_4, at variance with alkanes, readily interacts with MgO at room temperature.[28] The similar activation entropy decrements expected from the loss of transitional and rotational modes of the hydrocarbon moiety in the transition states of reactions 1 and 3 would be offset in the oxidation of a preequilibrated $C_2H_{4s} \leftrightarrow C_2H_4$(g) species in reaction 4. Previous reports based on atmospheric pressure experiments suggesting that $k_3 > k_1 > k_4$ are apparently incorrect.[26] Ethylene is oxidized faster than methane at accessible temperatures, despite having larger BDE(C−H) and activation energy values, for entropic reasons.

The van't Hoff parameters for K_1 and K_3 in Table 1 reveal that the O_s species responsible for ethane oxidation is as endothermic as that involved in reaction 1, but that ΔH_4 is about 17 kcal/mol larger than both. The positive entropy changes follow the same trend: $\Delta S_4 > \Delta S_1 \approx \Delta S_3$. We have argued that such parameters, contrary to the expected exothermicity of localized adsorption processes, actually imply cooperative participation of the solid.[12] In other words, the entropic driving force for chemisorption is provided by the concomitant restructuring of the catalyst.[37−39] We are currently developing a quantitative model accounting for these observations as well as for the results of unpublished $^{18}O_2$ labeling experiments on samaria.[40]

It is conceivable that the plots in Figures 5 and 6 were parallel lines having different intercepts. Such a case, not realized, would correspond to a unique O_s species possessing different reactivities toward the various hydrocarbons. Therefore, *the conclusion that the O_s species participating in reactions 1, 3, and 4 are kinetically and thermodynamically distinguishable is independent of any mechanistic assumption or proposed rate law. It is ultimately based on the quantitatively different phenomenological dependence of oxidation rates on $[O_2]$.* However, since we are dealing with thermal averages, the different O_s entities should not be necessarily construed as representing a discrete set of selective species.

In principle, measured rate constants for ethane and ethylene heterogeneous oxidations should be scaled to unit area of catalyst. Such scaling is always uncertain, because active areas are in general reaction sensitive and therefore not transferable. The use of BET areas is even more questionable under low pressure conditions, because, unless they become adsorbed, reactant molecules can hardly explore catalyst pores having dimensions much smaller than mean free paths.[12] Since our ultimate goal is to use present data in the kinetic analysis of the oxidative coupling of methane, we avoided this limitation by normalizing k_3 and k_4 values to the rate constants for methane oxidation k_1 measured on the same catalyst, either simultaneously or in back-to-back experiments. The basic assumption underlying this scaling procedure is that the steady state distribution of surface sites active in steps 1, 3, and 4 is independent of the catalyst history or morphology. This assumption is certainly less objectionable than those invoking active areas determined by other methods or under different experimental conditions. Equations I and II, lead to reactivity ratios: $k_3(C_2H_6)/k_1(CH_4) = 3.1 \pm 0.5$, and $k_4(C_2H_4)/k_1(CH_4) = 2.7 \pm 0.4$, at 1000 K, where the errors correspond to 95% confidence intervals.

The general validity of present results and conclusions may be gleaned from the fact that similar rate laws and parameters were obtained for the low pressure oxidations of methane on samaria and 7% Li-doped MgO,[11,12] for the formation of methyl radicals on Sr-doped La_2O_3,[10] and for the oxidations of ethane and ethylene on samaria. Endothermic O_2-chemisorption is also a common feature of all studies. These facts suggest that the role of catalyst oxides is to provide a substrate for O_2(g) activation and that their chemical composition may only affect the extent but not the nature of this process.[3,17−19,41] The apparent ceiling to C_2 selectivities of ca. 25% observed over a myriad of catalytic materials supports this conjecture.[1] Therefore, *optimization of C_2-yields in the oxidative dimerization of methane catalyzed by metal oxides may ultimately turn out to be a kinetic rather than a structural problem*.[12,18,30]

In principle, present results seem to agree with previous work on the oxidative dehydrogenation of C_2H_6 on Li/MgO regarding the fact that C_2H_4, its main reaction product,[24,25] is about three times less reactive than ethane at 824 K cf. Table 1.[24] Moreover, they apparently confirm isotope labeling experiments indicating that the oxidation of C_2H_4 is the main source of carbon oxides in methane oxidative dimerization.[16] However, as pointed out above, the accord should not be uncritically pressed further because atmospheric pressure experiments necessarily reflect the irreducible interplay between gas-phase and surface events and, therefore, can only approach present results under certain conditions.

Conclusions

The mechanism of the heterogeneous oxidations of ethane and ethylene on samaria is similar to the one previously found for the oxidations of methane and methyl radicals. Endothermic O_2 dissociative chemisorption creates distinguishable surface species possessing different reactivities toward each hydrocarbon. Ethane and ethylene are oxidized faster than methane under most experimental conditions, although the activation energies for the rate determining steps increase with R−H bond energies The main reaction pathway for ethane oxidation is dehydrogenation into ethylene mediated by ethyl radicals. Ethylene is oxidized to carbon monoxide.

Acknowledgment. This project was financially supported by CONICET/Argentina, under Grant PID/1131-91.

Appendix

It is instructive to compare the ethylene yields measured in the oxidation of ethane under the conditions of Figures 1 and 2, with those estimated on the basis of the evaluated rate constants k_3 and k_4. By assuming that (1) $\delta = 1$ in reaction 3, (2) reaction 6a is much faster than reaction 6b, and (3) CO_x species are only formed in reaction 4, we estimate a (63 ± 3)% ethylene yield for the experiment of Figure 2, instead of the observed 32% value. This is a significant discrepancy that deserves explanation. Notice that the first assumption is consistent with the lower CO_x yields found at the smaller conversion of Figure 1. In other words, carbon oxides must be formed at some stage after ethane consumption but before ethylene oxidation. Clearly, this apparent paradox really implies that C_2H_5(g) is rapidly oxidized to carbon oxides on the catalyst surface in competition with its gas-phase unimolecular decomposition. It can be shown that ethyl radical decomposition occurs in its second order region at the gas-wall collision frequencies attaining under present very low pressure conditions, with k_{6a} [M] ≈ 5 s^{-1}, [33−35,42] and that the 32% ethylene yield can be accounted for provided that $k_{6b} \approx k_{6a}$ at $[O_2] = 40$ nanomolar. This value of k_{6b} is consistent with a reaction probability per collision on the catalyst surface of about $\gamma_{6b} \approx 0.014$ at 1000 K. Observe that the condition $k_{6a} \gg k_{6b}$ will always apply at atmospheric pressures.

JA961273Q

(37) (a) Somorjai, G. A. *Annu. Rev. Phys. Chem.* **1994**, *45*, 721. (b) Gai, P. L.; Kourtakis, K. *Science*, **1995**, *267*, 661. (c) Borg, R. J.; Dienes, G. J. *The Physical Chemistry of Solids*; Academic: San Diego, 1992; Chapter 10.

(38) Levine, R. D. *Catal. Lett.* **1991**, *9*, 231.

(39) Levine, R. D.; Somorjai, G. A. *Surf. Sci.* **1990**, *232*, 407.

(40) Amorebieta, V. T.; Colussi, A. J. manuscript in preparation.

(41) Hutchings, G. J.; Scurrell, M. S.; Woodhouse, J. R. *J. Chem. Soc., Chem. Commun.* **1988**, 253.

(42) Grela, M. A.; Colussi, A. J. *Int. J. Chem. Kinet.* **1987**, *19*, 839.